

Second-Order Statistics for Indoor Wireless Joint Fading/Shadowing Channels

Indrakshi Dey and P. Salvo Rossi

Abstract—In this letter, we consider the joint fading and two-path shadowing (JFTS) channel model, which has been found suitable for characterizing indoor large open office environments with low mobility and stationary users. We derive useful expressions of fundamental channel statistics such as the number of level crossings in time, frequency, and space as well as average fade duration, bandwidth, and length for the JFTS faded/shadowed link. We also compare numerical results and their impact on system design over a variety of realistic propagation scenarios, which can be modeled by varying the JFTS parameters.

Index Terms—Average fade duration (AFD), indoor radio propagation, level-crossing rate (LCR), second-order statistics.

I. INTRODUCTION

A N APPROPRIATE composite fading/shadowing channel model that characterizes the transition from local small-scale fading to global shadowing statistics for indoor WLAN users is proposed in [1]. A joint distribution called the joint fading and two-path shadowing (JFTS) distribution that combines Ricean fading and the two-wave with diffused power (TWDP) shadowing model is shown to fit the measurement data. First-order statistical characterization of the received signal envelope over a JFTS faded/shadowed link is presented in [2]. The work in [3] derives expression for outage probability over a JFTS channel suffering from self-interference, which revealed that outage probability over a JFTS channel increases with the correlation between the desired and interfering signals, a trend opposite to traditional fading (e.g., Rayleigh, Nakagami) channel models in an interference-limited environment.

Focusing on second-order statistics, the level-crossing rate (LCR) determines the expected rate (number of crossings per second) at which the normalized channel process falls below a certain threshold, and the average fade duration (AFD) quantifies the amount of time that the received envelope spends underneath this threshold level once crossed. Such metrics are crucial to the design and performance evaluation of techniques such as multihop communications, diversity combining, etc. [4], [5].

In indoor wireless environments, users generally confine themselves within small coverage areas due to the incapability of most WLAN standards in handling hand-offs. Hence, the communication link can be considered to be quasi-static, and in that case, we may also define LCRs in terms of crossings

Manuscript received November 11, 2016; accepted December 14, 2016. Date of publication January 10, 2017; date of current version June 12, 2017. This work was supported in part by the European Research Consortium for Informatics and Mathematics (ERCIM) within the Alain Bensoussan Fellowship Program.

The authors are with the Department of Electronics and Telecommunications, Norwegian University of Science and Technology, Trondheim 7491, Norway (e-mail: indrakshi.dey@ntnu.no; salvorossi@ieee.org).

Color versions of one or more of the figures in this letter are available online at <http://ieeexplore.ieee.org>.

Digital Object Identifier 10.1109/LAWP.2017.2651153

per hertz, i.e., level crossings in frequency (LCF) and average fade bandwidth (AFB). The angular spectrum can be defined exclusively in terms of shape factors (angular spread, angular constriction, and direction of maximum fading) and used to do level crossing analysis on a quasi-static narrowband received envelope as a function of space [6]. In this case, the level crossings and the average fade component are termed level crossing in space (LCS) and average fade length (AFL), respectively.

In this letter, we focus on the second-order statistics of the JFTS distribution, for which we determine the approximate analytical solutions of its LCR, LCF, and LCS, and AFD, AFB, and AFL. These parameters also enable us to evaluate the impact of different propagation scenarios on the design requirements of different communication techniques (e.g., error-correction coding, spectral diversity, frequency hopping). For example, numerical results derived here show that as the user approaches the coverage boundary, fades on average occur almost five times more frequently, each lasting for only 3–10 times less than when the user is at the center of the coverage area of an access point. This results in wiping out 50% of the transmitted packets and can only be somewhat salvaged by increasing interleaving frequency by five times on average.

II. JFTS CHANNEL MODEL

The JFTS faded/shadowed signal envelope $Z(t)$ can be modeled as the product of two independent random processes, the small-scale fading process, $X(t)$, modeled using the Rician distribution, and the large-scale shadowing process, $Y(t)$, modeled using the TWDP distribution. The first-order statistics of the fading process is therefore given by

$$f_X(x) = \frac{x}{P_1} e^{-\frac{x^2}{2P_1} - K} I_0\left(x\sqrt{\frac{2K}{P_1}}\right) \quad (1)$$

where $I_0(\cdot)$ is the zeroth-order modified Bessel function of the first kind. The parameter K is the Rician K -factor, and P_1 is the mean-squared amplitude of the diffused components. On the other hand, the probability density function (PDF) of the shadowing process is

$$f_Y(y) = \frac{y}{P_2} e^{-\frac{y^2}{2P_2} - \sigma} \sum_{i=1}^4 \frac{a_i}{2} \left[I_0(y\sqrt{2\sigma(1 - \Delta T_i)/P_2}) + e^{\sigma\Delta T_i} + e^{-\sigma\Delta T_i} I_0(y\sqrt{2\sigma(1 + \Delta T_i)/P_2}) \right] \quad (2)$$

where $T_i = \cos((i - 1)\pi/7)$. The value of the shadowing parameter σ is based on the range of the discrete shadowing values experienced by a user while traveling through different scattering clusters. The shape parameter Δ of the shadowing distribution is based on the transition from one scattering cluster to the next one. The parameter P_2 is the mean-squared amplitude of

the shadowed components, and $a_1 = \frac{751}{17280}$, $a_2 = \frac{3577}{17280}$, $a_3 = \frac{49}{640}$, and $a_4 = \frac{2989}{17280}$ for $i = 1, 2, 3, 4$. Combining (1) and (2), the JFTS faded/shadowed envelope PDF, $f_Z(z)$, is given by [1]

$$\begin{aligned} f_Z(z) &= \sum_{i=1}^4 \frac{b_i z e^{-K-\sigma}}{2P_1 P_2} \sum_{h=1}^m R_h e^{-\frac{z^2}{2P_2 r_h^2}} \\ &\times [e^{\sigma \Delta T_i} I_0(2z\sqrt{K\sigma(1-\Delta T_i)/(P_1 P_2)}) \\ &+ e^{-\sigma \Delta T_i} I_0(2z\sqrt{K\sigma(1+\Delta T_i)/(P_1 P_2)})] \end{aligned} \quad (3)$$

where m is the quadrature order (determining approximation accuracy), $R_h = \frac{w_h}{|r_h|} e^{r_h^2(2P_1-1)/(2P_1)}$, and $b_i = a_i I_0(1)$. The multiplier w_h denotes the Gauss–Hermite quadrature weight factors, which is tabulated in [7] and is given by $w_h = (2^{m-1} m! \sqrt{\pi}) / (m^2 [H_{m-1}(r_h)]^2)$, where $H_{m-1}(\cdot)$ is the Gauss–Hermite polynomial with roots r_h for $h = 1, 2, \dots, m$. For our analysis, we have chosen $m = 20$.

III. SECOND-ORDER ENVELOPE STATISTICS

The LCR $N_t(Z)$ for a general time-varying process is a function of time and can be computed as [8], $N_t(Z) = \int_0^\infty \dot{z} f_{Z\dot{Z}}(z, \dot{z}) dz$ for $Z \geq 0$, where $f_{Z\dot{Z}}(z, \dot{z})$ is the joint PDF of $Z(t)$ and $\dot{Z}(t) = dZ(t)/dt$. The AFD can be given by $\bar{t}(Z_{\text{th}}) = \frac{F(Z_{\text{th}})}{N_t(Z_{\text{th}})}$, where Z_{th} is the specified threshold, and $F_Z(Z_{\text{th}}) = \int_0^{Z_{\text{th}}} f_Z(z) dz$ and $f_Z(z)$ are the corresponding envelope cumulative distribution function (CDF) and PDF, respectively. For a composite faded/shadowed signal envelope, the joint PDF of the signal envelope and its time derivative can be calculated as [9]

$$\begin{aligned} f_{Z\dot{Z}}(z, \dot{z}) &= \int_0^\infty \frac{1}{y^2} \left\{ \int_{-\infty}^\infty f_{X\dot{X}}\left(\frac{z}{y}, \frac{\dot{z}}{y} - \frac{\dot{y}z}{y^2}\right) \right. \\ &\times f_{Y\dot{Y}}(y, \dot{y}) dy \left. \right\} dy \end{aligned} \quad (4)$$

for $z \geq 0, -\infty \leq \dot{z} \leq \infty$. Using (4), we can derive mathematically tractable expressions for LCR and AFD of a JFTS faded/shadowed envelope.

Assuming a symmetrical power spectral density of X , the joint PDF $f_{X\dot{X}}(x, \dot{x})$ of a Rician fading process can be derived as [10]

$$f_{X\dot{X}}(x, \dot{x}) = 2A_1 x e^{-x^2 A_2 - \dot{x}^2 A_3} I_0(2xA_4) \quad (5)$$

where $A_1 = \frac{e^{-2K/(P_1(K+1))}}{P_1^{3/2}(K+1)^{3/2}\sqrt{\pi}\xi_\omega}$, $A_2 = 1/(P_1(K+1))$, $A_3 = 1/(\xi_\omega^2 P_1(K+1))$, and $A_4 = \sqrt{K/(P_1(K+1))}$. In this case, $\rho(t) = J_0(2\pi f_m t)$ is the correlation function for equal-amplitude incoming multipath waves with independent phases, where $J_0(\cdot)$ is the zeroth-order Bessel function of the first kind and f_m is the maximum Doppler shift. The corresponding correlation coefficients can be calculated as $\rho(0) = 1$ and $\rho''(0) = -2(\pi f_m)^2 = -\xi_\omega^2$, where ξ_ω is the corresponding root-mean-squared (RMS) Doppler spread.

Assuming that the TWDP distributed shadowing process Y is a sum of two power-symmetrical half-Rician processes [11], the joint PDF $f_{Y\dot{Y}}(Y, \dot{Y})$ of a TWDP-distributed shadowing

process can be derived as [12]

$$\begin{aligned} f_{Y\dot{Y}}(y, \dot{y}) &= \sum_{i=1}^4 \frac{a_i}{2} \left[2B_{1i} y e^{-y^2 B_{2i} - \dot{y}^2 B_{3i}} I_0(2yB_{4i}) \right. \\ &\left. + 2C_{1i} y e^{-y^2 C_{2i} - \dot{y}^2 C_{3i}} I_0(2yC_{4i}) \right] \end{aligned} \quad (6)$$

where $B_{1i} = \frac{e^{-2\sigma(1-\Delta T_i)/(P_2(\sigma(1-\Delta T_i)+1))}}{P_2^{3/2}(\sigma(1-\Delta T_i)+1)^{3/2}\sqrt{\pi}\zeta}$, $B_{2i} = 1/(P_2(\sigma(1-\Delta T_i)+1))$, $B_{3i} = 1/(\zeta^2 P_2(\sigma(1-\Delta T_i)+1))$, $B_{4i} = \sqrt{\frac{\sigma(1-\Delta T_i)}{P_2(\sigma(1-\Delta T_i)+1)}}$, $C_{1i} = \frac{e^{-2\sigma(1+\Delta T_i)/(P_2(\sigma(1+\Delta T_i)+1))}}{P_2^{3/2}(\sigma(1+\Delta T_i)+1)^{3/2}\sqrt{\pi}\zeta}$, $C_{2i} = 1/(P_2(\sigma(1+\Delta T_i)+1))$, $C_{3i} = 1/(\zeta^2 P_2(\sigma(1+\Delta T_i)+1))$, and $C_{4i} = \sqrt{\frac{\sigma(1+\Delta T_i)}{P_2(\sigma(1+\Delta T_i)+1)}}$. In this case, $\psi(t) = e^{-2(\pi\xi_s t)^2}$ is the covariance function for the shadowing process, where $\xi_s = f_s/(\sqrt{2 \ln 2})$ and f_s is the 3-dB cutoff frequency. The corresponding covariance coefficients can be calculated as $\psi(0) = 1$ and $\psi''(0) = -2(\pi\xi_s)^2 = -\zeta^2$.

A. Envelope LCR, LCF, and LCS

By substituting (5) and (6) in (4), the integral solution from [13, eq. (3.321.3), p. 336] and Laguerre–Gauss quadrature method, we can obtain the final expression for LCR in JFTS channels as (see the Appendix)

$$\begin{aligned} N_t(Z) &= \sum_{i=1}^4 \sum_{j=1}^n \frac{a_i A_1 z y_j I_0\left(\frac{2A_4 z}{y_j}\right) \sqrt{\pi}}{(n+1)^2 [\mathcal{L}_{n+1}(y_j)]^2} \left[\frac{2B_{1i} e^{y_j - y_j^2 B_{2i} - \frac{A_2 z^2}{y_j^2}}}{\sqrt{A_3 z^2 + B_{3i} y_j^4}} \right. \\ &\times \left(\frac{z^2}{2y_j^2 B_{3i}} + \frac{y^2}{2A_3} \right) I_0(2y_j B_{4i}) + \frac{2C_{1i} e^{y_j - y_j^2 C_{2i} - \frac{A_2 z^2}{y_j^2}}}{\sqrt{A_3 z^2 + C_{3i} y_j^4}} \\ &\times \left. \left(\frac{z^2}{2y_j^2 C_{3i}} + \frac{y^2}{2A_3} \right) I_0(2y_j C_{4i}) \right] \end{aligned} \quad (7)$$

for $(A_3 z^2 / y^4 + B_{3i}) > 0$, $(A_3 z^2 / y^4 + C_{3i}) > 0$, where $\mathcal{L}_\xi(\cdot)$ is the Laguerre polynomial. Applying duality, $\xi_\omega \rightarrow 2\pi\xi_\tau$, the LCF for frequency selective channels, $N_f(Z)$, can be written in the form of (7) just by replacing (A_1, A_3) with (A_5, A_6) , where ξ_τ is the delay spread and $A_5 = \frac{e^{-2K/(P_1(K+1))}}{P_1^{3/2}(K+1)^{3/2}2\pi^3/\xi_\tau}$, $A_6 = \frac{1}{(2\pi\xi_\tau)^2 P_1(K+1)}$. Applying duality $\xi_\omega \rightarrow \xi_\kappa$, LCS $N_\kappa(Z)$ can be written in the form of (7) just by replacing (A_1, A_3) with (A_7, A_8) , where ξ_κ is the wavenumber spread given by $\xi_\kappa^2 = \frac{2\pi^2 \Lambda^2}{\lambda^2} (1 + \gamma \cos[2(\theta_R - \theta_{\max})])$ [6], and $A_7 = \frac{\lambda e^{-2K/(P_1(K+1))}}{P_1^{3/2}(K+1)^{3/2}\Lambda\pi^{3/2}\sqrt{2+2\gamma\cos[2(\theta_R - \theta_{\max})]}} A_8 = \frac{\lambda^2}{(2\pi^2 \Lambda^2 (1 + \gamma \cos[2(\theta_R - \theta_{\max})])) P_1(K+1)}$. Here, λ is the wavelength of carrier frequency, Λ is the angular spread, γ is the reflected and shadowed multipath angular constriction values, θ_R is the azimuthal direction, and θ_{\max} is the azimuthal direction of maximum composite fading/shadowing.

B. Envelope AFD, AFB, and AFL

In order to compute the average AFD, we first of all need to derive the CDF of the JFTS envelope process. By definition, the expression for JFTS CDF can be determined as $F_Z(z) = \int_{-\infty}^z f_U(u) du$, where U is the JFTS distributed received signal

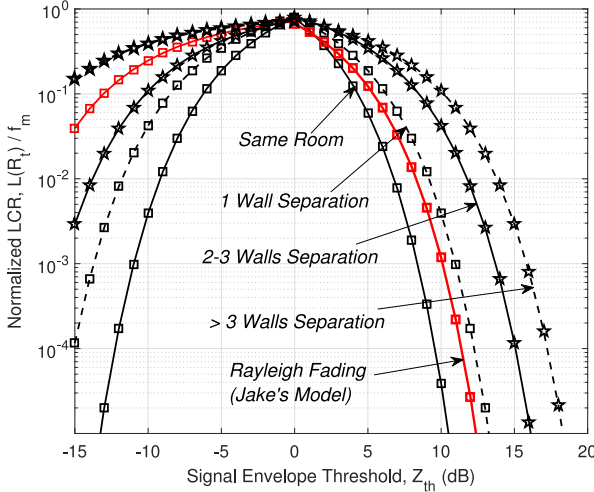


Fig. 1. Normalized LCR versus envelope threshold level in JFTS faded/shadowed communication link, where the curves are generated by varying all the JFTS parameters, K , σ , and Δ simultaneously. Normalized LCR over Rayleigh channel is also plotted for comparison.

envelope with PDF given by (3). Using the integral solution from [13] and the Marcum Q -function, we can represent the expression for the CDF of the JFTS envelope process as

$$F_Z(z) = \sum_{i=1}^4 \sum_{h=1}^m \frac{b_i}{2} \frac{R_h r_h e^{-K-\sigma}}{P_1 \sqrt{P_2}} \left[Q_1 \left(\sqrt{\frac{K\sigma}{P_1}} (1 - \Delta T_i r_h), z \right) \right. \\ \left. \times e^{\sigma \Delta T_i} + e^{-\sigma \Delta T_i} Q_1 \left(\sqrt{\frac{K\sigma}{P_1}} (1 + \Delta T_i r_h), z \right) \right] \quad (8)$$

where Q_1 is the Marcum Q -function, monotonic and log-concave in statistical characteristics. Finally, the expression for AFD in JFTS faded/shadowed communication channels can be obtained by substituting (7) and (8) in the general expression for AFD. Similarly, the expression for AFB, $\bar{f}(Z_{th}) = \frac{F(Z_{th})}{N_f(Z_{th})}$ can be calculated from (8) and (10), while the expression for AFL $\bar{\kappa}(Z_{th}) = \frac{F(Z_{th})}{N_\kappa(Z_{th})}$ can be calculated from (8) and (10).

IV. SIMULATION RESULTS AND DISCUSSION

A. Numerical Analysis

The results in Figs. 1 and 2 are generated by varying the JFTS parameters K , σ , and Δ simultaneously. The values for each set of parameters are chosen from the ranges of their numerical values proposed in [1], depending on the relative position of the mobile LAN user and the access point. The first curves in both figures are generated for $K = 10$ dB, $\sigma = 10.5$ dB, and $\Delta = 0.75$, representing a condition where both the user and the access point are located in the same room. As the user moves to a different room separated by one set of wall or partition from that of the access point ($K = 8$ dB, $\sigma = 6.5$ dB, and $\Delta = 0.45$), the LCR increases along with the AFD as exhibited by the second curves in Figs. 1 and 2. It should be emphasized that we assume common path loss for all four scenarios. This means that all four scenarios experience the same average path loss, and the difference in LCR and AFD shown on plots is a result of the different fading and shadowing statistics imposed by the JFTS model.

The LCR and AFD over a JFTS distributed channel gets higher than the conventional Rayleigh fading case with isotropic

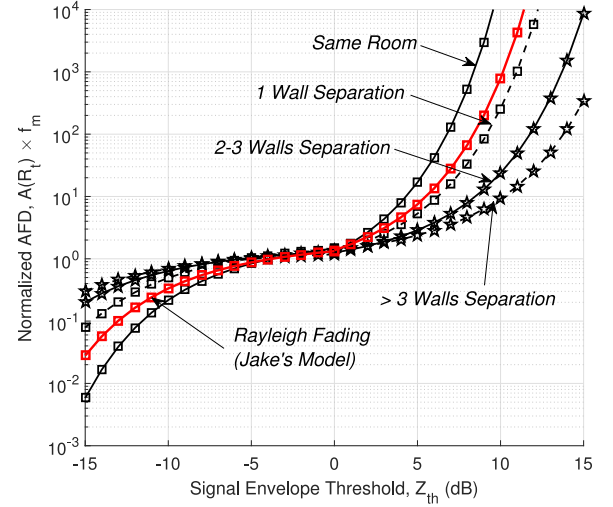


Fig. 2. Normalized AFD versus envelope threshold level in JFTS faded/shadowed communication link, where the curves are generated by varying all the JFTS parameters K , σ , and Δ simultaneously. Normalized AFD over Rayleigh channel is also plotted for comparison.

TABLE I
SYSTEM SPECIFICATIONS

Transmission rate	:	1 data packet every 20 ms
Doppler spread	:	10 Hz
Threshold for received signal (Z_{th})	:	$10 \text{ dB} \approx \sqrt{0.1}$

scattering as soon as the user and the access point are separated by one set of wall or partition (see Figs. 1 and 2). The only exception is the LCR exhibited over the signal level range lower than 0 dB. The reason for this behavior can be that the JFTS distribution still presents a very small group of specular components as long as $K \neq 0$. Meanwhile, for the Rayleigh fading case, $K = 0$ with the absence of any specular component provides poor performance with lower signal level.

Propagation conditions deteriorate even further, if the user and the access point are separated by two to three sets of dry-walls ($K = 6.5$ dB, $\sigma = -1.5$ dB, and $\Delta = 0.25$) and more than three sets of partitions ($K = 5.5$ dB, $\sigma = -7.5$ dB, and $\Delta = 0.15$). This happens due to the lack of strong specular components and the presence of at least two scattering clusters between the transmitter and the receiver, which jointly deteriorates the overall system performance.

B. Impact on System Design

1) *Level Crossing:* We consider a narrowband wireless system employing error-correction coding with details in Table I. Using this system information and (7), we can find out the rate of information loss over a variety of realistic environments modeled using JFTS parameters. A summary of their corresponding LCRs and worst-case scenarios in terms of data loss are tabulated in Table II.

2) *Fade Duration:* We assume the communication scenario presented in Table III, where a mobile user is walking towards an access point inside a big office building. Using the system and link specifications in Table III, we can calculate the AFD [see (8)] and then use it to calculate the corresponding suitable interleaving time for different ranges of the JFTS parameters, which are tabulated in Table IV.

TABLE II
THEORETICAL LCRS FOR JFTS DISTRIBUTION

JFTS parameters	LCR (crossings/sec)	Avg. time per crossing (ms)	Worst case scenario
Same room	3.65 to 6.32	160 to 280	One packet wiped out in every eight packets
1 wall partition	7.91 to 12.78	78 to 126	One packet wiped out in every five packets
2/3 wall partitions	13.63 to 15.8	63 to 72	One packet wiped out in every three packets
> 3 wall partitions	16.27 to 23.4	43 to 61	One packet wiped out in every two packets

TABLE III
COMMUNICATION SCENARIO

Mobile user velocity (v)	:	1.25 m/s
Carrier Frequency (f_c)	:	2.45 GHz
RMS signal-to-noise ratio (SNR)	:	10 dB
Threshold SNR with noise variance ν^2 ($\frac{v^2}{2\nu^2}$)	:	3 dB
Threshold for received signal (Z_{th})	:	$\sqrt{0.6}$
Channel coherence time	:	12.5 ms
Transmission symbol rate	:	0.25 Msps

TABLE IV
THEORETICAL AFDs FOR JFTS DISTRIBUTION

JFTS parameters	AFD (ms)	Interleaving symbols
Same room	80 to 90	64 to 72
1 wall partition	68.7 to 81.2	55 to 65
2/3 wall partitions	38.7 to 61.4	31 to 49
> 3 wall partitions	7.5 to 33.6	6 to 27

V. CONCLUSION

In this letter, we derived new expressions for second-order statistics such as the LCR, LCF, and LCS as well as AFD, AFB, and AFL of the JFTS faded/shadowed wireless communication link. Using these expressions, we plotted numerical results and investigated their impact on system design over a variety of propagation scenarios by varying the JFTS parameters. The results demonstrated that both the LCR and AFD increase with the number of separations or dry-walls between the access point and the mobile WLAN user in large open indoor wireless propagation scenarios.

APPENDIX DERIVATION OF LCR

By substituting (5) and (6) in (4), and then using the integral solution from [13, eq. (3.462.2), p. 365], we can obtain

$$\begin{aligned} \int_{-\infty}^{\infty} f_{X \dot{X}} \left(\frac{z}{y}, \frac{\dot{z}}{y} - \frac{\dot{y}z}{y^2} \right) f_{Y \dot{Y}} (y, \dot{y}) dy &= \sum_{i=1}^4 2a_i A_1 z e^{-\frac{z^2}{y^2} A_2} \sqrt{\pi} \\ &\times e^{-\frac{\dot{z}^2}{y^2} A_3} I_0 \left(\frac{2z}{y} A_4 \right) \left[\frac{B_{1i} y^2 e^{-y^2 B_{2i}}}{\sqrt{A_3 z^2 + B_{3i} y^4}} e^{\frac{A_3^2 z^2 \dot{z}^2}{y^2 (A_3 z^2 + B_{3i} y^4)}} \right. \\ &\times I_0(2yB_{4i}) + \left. \frac{C_{1i} y^2 e^{-y^2 C_{2i}}}{\sqrt{A_3 z^2 + C_{3i} y^4}} I_0(2yC_{4i}) e^{\frac{A_3^2 z^2 \dot{z}^2}{y^2 (A_3 z^2 + C_{3i} y^4)}} \right]. \end{aligned} \quad (9)$$

Using (9) in (4), then putting it back in the general expression for LCR, and finally using the integral solution from [13, eq. (3.321.3), p. 336], we can obtain the final expression for LCR in JFTS faded/shadowed communication links as

$$\begin{aligned} N_t(Z) = \sum_{i=1}^4 a_i A_1 z \int_0^{\infty} e^{-\frac{A_2 z^2}{y^2}} I_0 \left(2A_4 \frac{z}{y} \right) \\ \times \left[\frac{2B_{1i} \sqrt{\pi} e^{-y^2 B_{2i}}}{\sqrt{A_3 z^2 + B_{3i} y^4}} \left(\frac{z^2}{2y^2 B_{3i}} + \frac{y^2}{2A_3} \right) I_0(2yB_{4i}) \right. \\ \left. + \frac{2C_{1i} \sqrt{\pi} e^{-y^2 C_{2i}}}{\sqrt{A_3 z^2 + C_{3i} y^4}} \left(\frac{z^2}{2y^2 C_{3i}} + \frac{y^2}{2A_3} \right) I_0(2yC_{4i}) \right] dy \end{aligned} \quad (10)$$

for $(A_3 z^2 / y^4 + B_{3i}) > 0$, $(A_3 z^2 / y^4 + C_{3i}) > 0$. Using Laguerre–Gauss Quadrature method, we can arrive at an approximate form of (10) as (7) or, alternatively, can evaluate the integral in (10) numerically to desired accuracy using MATLAB and MATHEMATICA. Further normalizing (10) with respect to f_m will make the LCR of a JFTS faded/shadowed envelope independent of the mobile user's velocity.

REFERENCES

- [1] I. Dey, G. G. Messier, and S. Magierowski, "Joint fading and shadowing model for large office indoor WLAN environments," *IEEE Trans. Antennas Propag.*, vol. 62, no. 4, pp. 2209–2222, Apr. 2014.
- [2] I. Dey, G. G. Messier, and S. Magierowski, "Fading statistics for the joint fading and two path shadowing channel," *IEEE Wireless Commun. Lett.*, vol. 3, no. 3, pp. 301–304, Jun. 2014.
- [3] I. Dey and P. Salvo Rossi, "Probability of outage due to self-interference in indoor wireless environments," *IEEE Commun. Lett.*, vol. 21, no. 1, pp. 8–11, Jan. 2017. doi: 10.1109/LCOMM.2016.2613979.
- [4] X. Dong and N. C. Beaulieu, "Average level crossing rate and average fade duration of selection diversity," *IEEE Commun. Lett.*, vol. 5, no. 10, pp. 396–398, Oct. 2001.
- [5] N. Zlatanov, Z. Hadzi-Velkov, and G. K. Karagiannidis, "Level crossing rate and average fade duration of the double Nakagami- m random process and application in MIMO keyhole fading channels," *IEEE Commun. Lett.*, vol. 12, no. 11, pp. 822–824, Nov. 2008.
- [6] G. D. Durgin and T. S. Rappaport, "Effect of multipath angular spread on the spatial cross-correlation of received voltage envelopes," in *Proc. IEEE Veh. Technol. Conf.*, Jul. 1999, pp. 996–1000.
- [7] M. Abramowitz and I. A. Stegun, *Handbook of Mathematical Functions with Formulas, Graphs, and Mathematical Tables*, 1972. New York, NY, USA: Dover.
- [8] G. L. Stuber, *Principles of Mobile Communications*, 2nd ed. Boston, MA, USA: Kluwer, 1996.
- [9] A. Krantzik and D. Wolf, "Distribution of the fading intervals of modified Suzuki process," *Signal Processing V: Theories and Applications*. Amsterdam, The Netherlands: Elsevier, 1990, pp. 361–364.
- [10] T. Eltoft, "The Rician inverse Gaussian distribution: A new model for non Rayleigh signal amplitude statistics," *IEEE Trans. Image Process.*, vol. 14, no. 11, pp. 1722–1735, Nov. 2005.
- [11] G. D. Durgin, T. S. Rappaport, and D. A. de Wolf, "New analytical models and probability density functions for fading in wireless communications," *IEEE Trans. Commun.*, vol. 50, no. 6, pp. 1005–1015, Jun. 2002.
- [12] M. Rao, F. J. Lopez-Martinez, and A. Goldsmith, "Statistics and system performance metrics for the two wave with diffuse power fading model," in *Proc. 48th Annu. IEEE Conf. Inf. Sci. Syst.*, 2014, pp. 1–6.
- [13] I. S. Gradshteyn and I. M. Ryzhik, *Table of Integrals, Series and Products*, 7th ed. New York, NY, USA: Academic.